International Journal of Engineering Trends and Technology
ISSN: 2231 – 5381 / https://doi.org/10.14445/22315381/IJETT-V71I2P239

Volume 71 Issue 2, 371-381, February 2023

Original Article

Gap Coupled Suspended Ultra-Wideband Microstrip Antennas for 5G Applications

Pradeep Reddy[1], Veeresh G Kasabegoudar[2]

[1,2]*ECE Department, Central University of Karnataka, Kalaburagi, India.*

[1]*Corresponding Author : pradeepmr056@gmail.com*

Received: 15 November 2022 Revised: 13 February 2023 Accepted: 18 February 2023 Published: 25 February 2023

Abstract *- This paper presents a new simple feeding technique suitable for suspended MSAs (microstrip antenna) with ultrawideband (UWB) performance. Antennas with the feed network presented here offer an impedance bandwidth (S_{11} < -10 dB) in excess of 50%. The antenna geometries demonstrated here are fed through a sub-miniature (SMA) connector, which is located aside the rectangular radiating element. The coaxial probe located off the radiating element supplies the energy to the main antenna element through a capacitive means. Of the two configurations demonstrated here to offer the return loss bandwidth of 52.83% (antenna 1) and 56.14% (antenna 2), respectively. The corresponding values of the measured results are 52.30% and 56.12%, respectively. Further, both cases presented here offer a gain of more than 5 dB and good radiation characteristics over the whole frequency band of interest. The antenna geometries presented here have been optimized with detailed parametric studies. Further, the experimental results presented here exhibit a good match with the simulated data.*

Keywords *- Gap coupled antenna, Suspended microstrip antenna, UWB antenna, 5th Generation (5G), LTE.*

1. Introduction

Low profile and single layer MSAs with wide and/or multi-band/frequency characteristics, good gain, and stable radiation parameters [1-7] are the most desirable antenna parameters in the 4th generation long term evolution (4G-LTE) and 5th generation (5G) wireless applications. However, microstrip antennas in their traditional form exhibit low bandwidth and low gain values. After the patch antennas' commencement, a lot of research has been reported to improve these parameters. Some of the well-known methods to enhance the characteristics of the antenna are the use of thick dielectric substrates [8], substrates suspended in air dielectric [7-19], modifying the shape of the radiating geometries [20-24], multilayer configurations [8], and modified or hybrid feed techniques [25-33] etc.

There are numerous bandwidth improvement methods available that include the alteration of the feeding structure, and changing the profile of the probe, such as L [25-27], meander [28], T [29], etc. Among the bandwidth enhancement methods, coupling the radiator patch through capacitive means is the most popular and has been demonstrated by several researchers [9-16] for enhancing the S_{11}<-10dB bandwidth. Since the coaxial probe-pin exhibits inductive reactance typically at the upper-frequency band of working is nullified by the capacitive coupling. The antenna presented in [10] offers a return loss bandwidth of 50%. Here, a small feed strip with a rectangular or circular shape is located 0.5 mm from the radiator patch along the length side. The feed strip acts as an active element since the coaxial pin is directly soldered to the feed patch, and the main antenna element is coupled capacitively to the feed patch. The main problem associated with this geometry is spurious radiation, especially at higher frequencies as the physical dimensions approach the wavelength of the frequency of operation. Besides this, the feed strip has to be redesigned as and when the frequency of operation is altered. Moreover, due to the small physical size, the feed strip causes soldering restrictions at the time of fabrication of the prototype. Therefore, this investigation focuses on eliminating the need for feed strips and keeping the antenna characteristics more or less similar. Additionally, an effort has been made to include the probe pin near the radiating patch, which greatly decreases the large space necessities for the presented antenna. Though, it must be noticed that the coaxial pin is yet placed away from the patch antenna. Comprehensive studies on parametric variations have been conducted to enhance the proposed antenna structures presented in the following paragraphs of this work.

Basic antenna structures and their optimized characteristics are presented in Section 2. A detailed parametric investigation is done to optimize the proposed antennas with gap-coupled feed is explained in Section 3. Measured & analysis of the results are explained in Section 4. The conclusion part of the work is given in Section 5.

2. Proposed Antenna Configuration

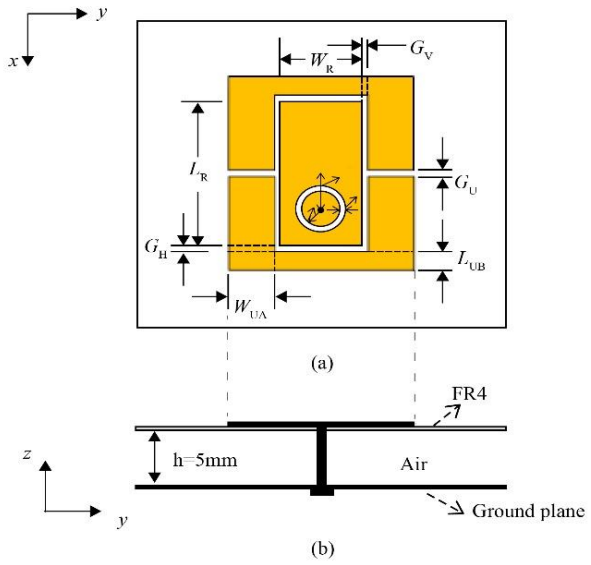

a) Capacitively coupled antenna with concentric ring [14]

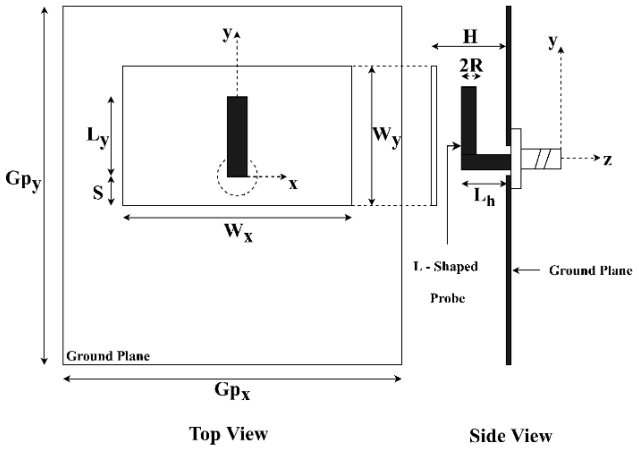

b) Capacitively coupled antenna with an L-shaped probe [24]

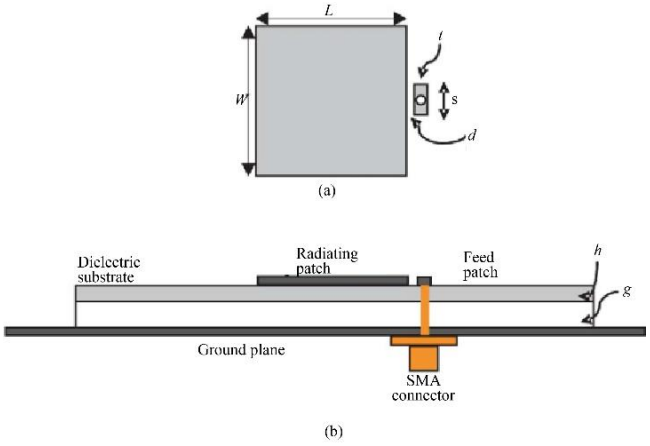

c) Capacitively coupled antenna through feed strip [10]

Fig 1. Typical capacitive coupled microstrip antennas

As stated earlier, several researchers have investigated the improvement of the conventional antenna with a capacitive feed. A few prominent capacitive coupled techniques reported in the literature are presented in Figure 1(A)-1(C).

The basic antenna design presented here and the initial airgap selection are similar to the geometry presented in [10]. The initial air gap value can be calculated from (1)

$$g = 0.16\lambda_c - h\sqrt{\varepsilon_r} \quad (1)$$

Further, the length of the patch (L) and width of the patch (W) is calculated from the well-known equations available for the design of a rectangular patch by taking the air gap into account, i.e., total height is equal to the sum of air gap & height of the substrate and, the effective dielectric constant of air-dielectric combination is calculated from [10]

$$\varepsilon_{re} = \frac{\varepsilon_r\left(1+\frac{g}{h}\right)}{1+\varepsilon_r\left(\frac{g}{h}\right)} \quad (2)$$

For simulation, the infinite ground is assumed and while fabrication, a finite ground of 10cmx10cm was used for prototype design. As explained in [10], the finite ground and/or substrate affect radiation patterns due to surface waves which affect the antenna's gain vs frequency characteristics. However, ground dimensions have a mere effect on return-loss characteristics. Although the ground size of λ x λ offers an optimum gain, the larger ground of about 2λ x 2λ was used to facilitate the radiation patterns measurements in an anechoic chamber.

Table 1. Physical dimensions of proposed antennas

Parameter	Work reported in [10]	Prop. antenna 1	Prop. antenna 2
Length of the patch (*L*)	15.50 mm	15.50 mm	15.50 mm
Width of the patch (*W*)	16.40 mm	16.40 mm	16.40 mm
Feed(strip) length(*s*)	3.70 mm	Not Applicable	Not Applicable
Feeding patch width(*t*)	1.20 mm	Not Applicable	Not Applicable
Probe pin position (*d*)	0.50 mm	0.40 mm	0.20 mm
Airgap (*g*)	6.00 mm	6.50 mm	5.50 mm

The proposed antenna geometries are shown in Figures 2 and 3 [15]. As mentioned earlier, the presented antenna's geometry is implemented from [10] but without a feed strip. The main purpose of removing the feed strip is that it makes the entire geometry asymmetrical, and also unwanted radiations may appear at high-frequency values.

Further, it poses physical limitations during implementation. Besides this, the feed patch has to be reoptimized when a different operation frequency is chosen. Hence, in this work, an effort has been made to eliminate it by retaining the antenna's performance the same as that of the antenna with a feed strip. The optimized characteristics of the proposed antenna are depicted in Table 1. The data values presented here are compared with the results of [10] to demonstrate the significance of the present work.

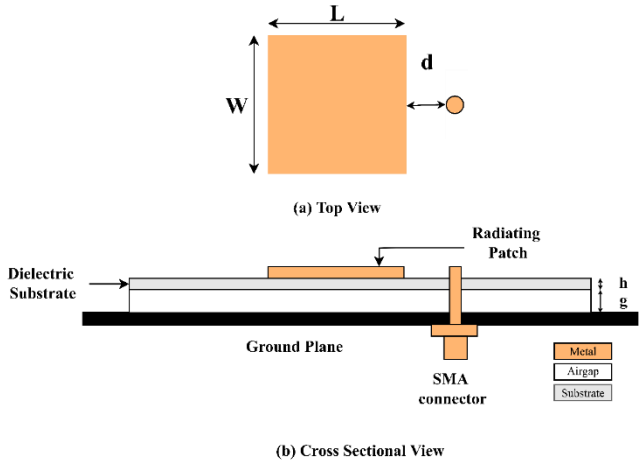

Fig. 2 Suspended MSA with probe-pin located away from the patch

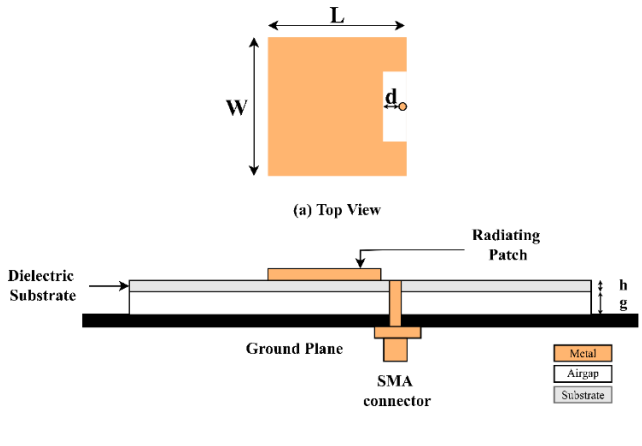

Fig. 3 Suspended MSA with probe-pin located inside the area of the patch

3. Design Optimization

This section covers the optimization of the antenna geometries with a novel feed. A detailed parametric study was conducted to arrive at the final design. It may be noted that after eliminating the feed strip reported in [10], the only parameters to be optimized are the separation between the radiating patch element & the probe pin (*d*), and the air gap (*g*), and. These are presented in the following subsections. Further, the variations of resistive and reactive components of the input impedance vs geometry parameters were found to comply with the results published in [10] and are presented at the end of this section.

3.1. Distance between Probe and the Patch Edge (d)

As explained earlier, in the first case, the probe pin is located at a distance of "d" mm from the patch's radiating edge (along the length side). It may be noted that the top view of the probe pin grazes the top surface of the substrate (patch side). In the second case, the patch's outer edge is modified so that the probe pin is located just inside the area of the rectangular patch with no physical contact. These two cases have been presented in the following subsections.

3.1.1 Geometry with Probe Feed Away from the Radiating Patch

In the first case investigated, the probe pin is located outside the patch, separated by '*d*' mm from the radiating edge of the rectangular patch. The parametric study was conducted on this parameter keeping the initial value of the air gap as 6.0 mm as suggested in [10]. The distance *d* was varied between 0.4 mm and 1.0 mm. The optimal value of the distance was found to be 0.4mm. For this value of *d*, the percentage of impedance bandwidth obtained is 52.83%. These values are presented in Table 2. From Table 2, it may be noticed that for an air gap of 6.5mm, an optimum distance of d=0.4 mm offers an impedance bandwidth of 52.83%. Return-loss parameters of the same are depicted in Figure 4.

Table 2. Percentage of bandwidth vs frequency for various values of 'd' for an airgap (g) of 6.5 mm

d (mm)	Bandwidth (GHz)	Percentage Bandwidth
0.4	2.85	52.83
0.5	2.86	52.63
0.6	2.88	52.62
0.7	2.87	52.32
0.8	2.88	52.02
0.9	2.87	51.84
1.0	2.87	51.61

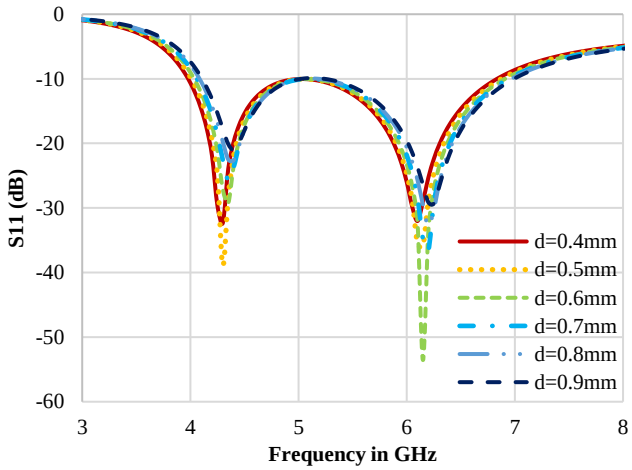

Fig. 4 Return-loss characteristics versus frequency for an air gap of 6.5 mm

Table 3. Percentage of bandwidth vs frequency for different values of 'd' for an air gap (g) of 5.5mm

d (mm) (from the inner edge)	Bandwidth (GHz)	Percentage Bandwidth
0.1	3.05	55.76
0.2	3.13	56.14
0.3	3.14	55.48
0.4	3.12	54.42
0.5	3.09	53.25
0.6	2.71	44.50
0.7	2.51	40.39
0.8	2.43	38.66
0.9	2.39	37.80

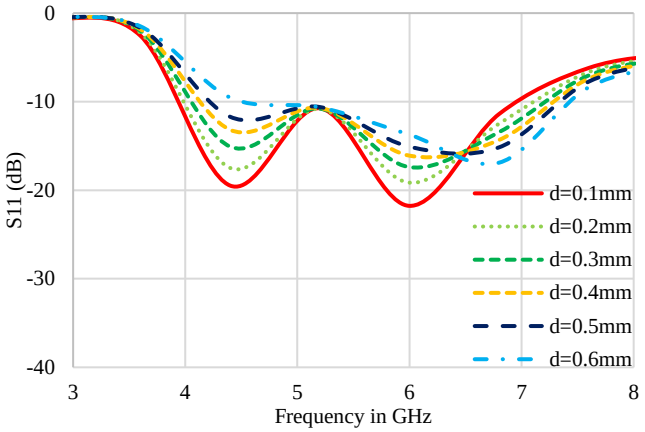

Fig. 5 Return-loss characteristics versus frequency for an air gap of 6.0mm for an antenna geometry 2

3.1.2 Geometry with Probe Feed inside the Radiating Patch

In another effort to make the geometry compact, the distance between the patch element and the feed probe was removed, and the probe pin was placed in the vicinity of the patch's inner edge. The modified geometry is shown in Figure 2. This geometry is much simpler compared to the original geometry reported in [10]. Similar to the geometry presented in Section 3.1.1, this antenna geometry also does not require the optimization of feed strip (*s* and *t*). Results obtained for different values of air gap are presented in Table 3. From Table 3, it is found that for an air gap of 5.5 mm with an optimum distance of d=0.2 mm, the proposed antenna offers an impedance bandwidth of 56.14%. The S_{11} parameters of the same are depicted in Figure 5.

3.2. Airgap Optimization

In this study, the amount of suspension above the ground plane or air gap between the ground and dielectric substrate was varied between 5.5 mm to 7.5 mm for antenna 1 and 5.0 mm to 7.0 mm for antenna 2 in steps of 0.5 mm and keeping the d value optimum (0.4 mm for case 1 and 0.2 mm for case 2) as obtained in the previous section. Return-loss values obtained for this study are shown in Figure 6(a).

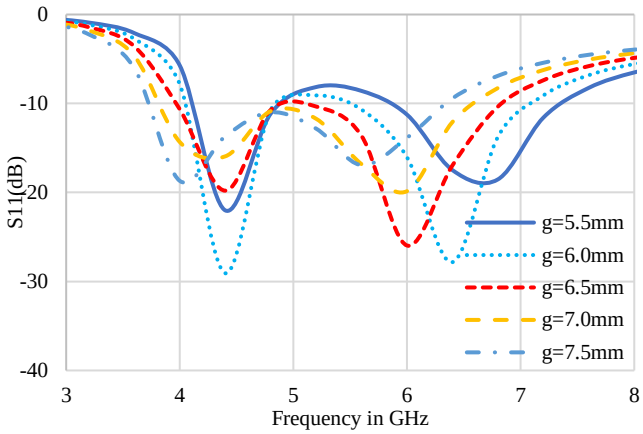

a) Return loss vs frequency characteristics for case 1 with d=0.6 mm

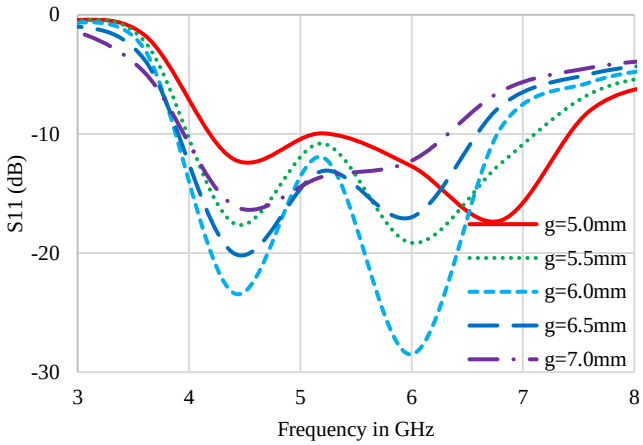

b) Return loss vs frequency characteristics for case 2 with d=0.5 mm

Fig 6. Antenna characteristics variations for different values of airgap

Similarly, for the second case investigated, the air gap was varied from 4mm to 7mm in steps of 1mm, and the characteristics obtained from the study are presented in Figure 6(b). For the proposed antenna geometries 1 and 2, the optimum air gap values were found to be 6.5 mm and 5.5 mm, and the corresponding bandwidth values obtained are 52.83% and 56.14%, respectively. The gain vs frequency plots is presented in Figure 7 for both antennas. It may be noted that the antenna's gain is almost the same for both cases presented and is above 5 dB throughout the working band.

Input impedance values vs frequency are presented in Figures 8 & 9 for different values of 'd' (distance between probe pin and the edge of the patch). From these characteristics, it may be noted that for both cases (antennas 1 and 2), the reactive part is capacitive below the centre frequency and becomes inductive above it. The reactive part is negligible at the centre frequency, and the real part is close to 50 Ohms. Further, input impedance values of proposed antennas are compared with the antenna presented in [10] and found to have similar performance. These characteristics are presented in Figure 10.

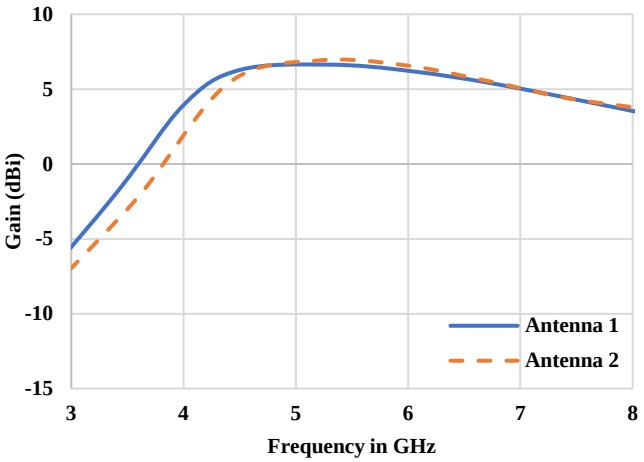

Fig. 7 Gain vs frequency characteristics for the proposed antennas

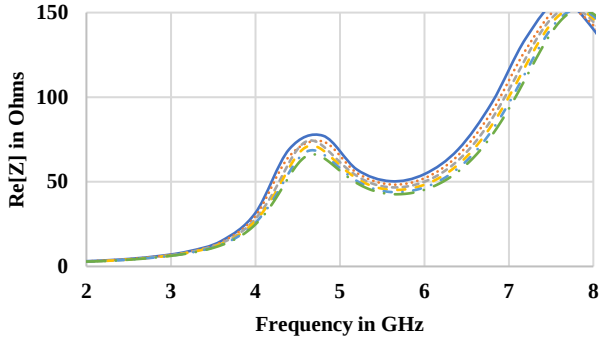

a) Re(Z) vs frequency plot for antenna geometry 1 for different values of d

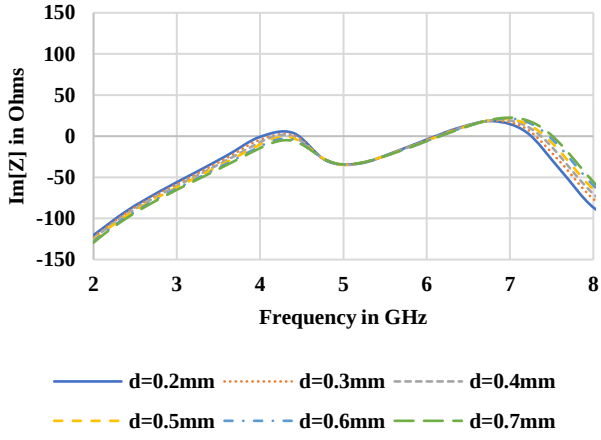

b) Im(Z) vs frequency plot for antenna geometry 1 for different values of d

Fig. 8 Impedance vs frequency characteristics for antenna geometry 1 for different values of d

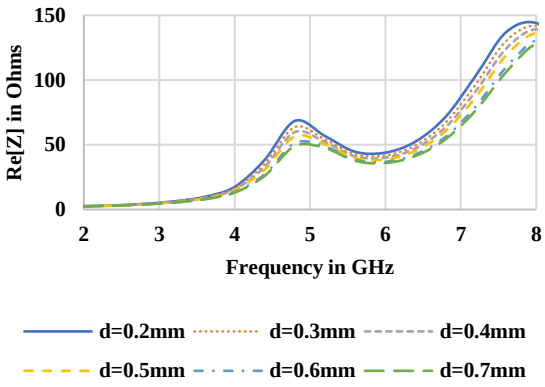

a) Re(Z) vs frequency plot for antenna geometry 2 for different values of d

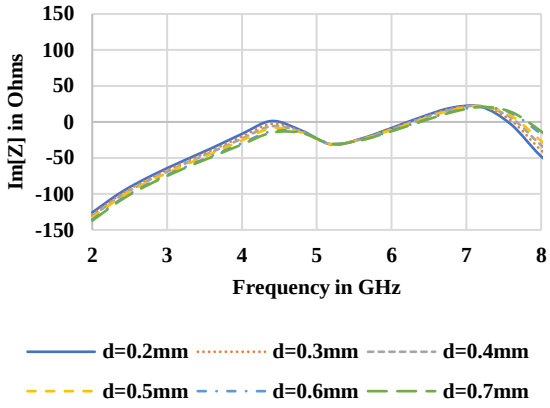

b) Im(Z) vs frequency plot for antenna geometry 2 for different values of d

Fig. 9 Impedance vs frequency characteristics for antenna geometry 2 for different values of d

Table 4. Percentage of bandwidth vs frequency for different values of 'g'

Proposed antenna geometry 1 (case 1) (d=0.4 mm)		Proposed antenna geometry 2 (case 2) (d=0.2 mm)	
Airgap (*g*) mm	**Percentage Bandwidth**	**Airgap (*g*) mm**	**Percentage Bandwidth**
5.5	18.65 and 23.81 (split/dual bands)	5.0	54.73 (Single band)
6.0	20.76 and 26.97 (split/dual bands)	5.5	56.14 (Single band)
6.5	53.36 (Single band)	6.0	54.37 (Single band)
7.0	52.82 (Single band)	6.5	53.41 (Single band)
7.5	52.03 (Single band)	7.0	47.95 (Single band)

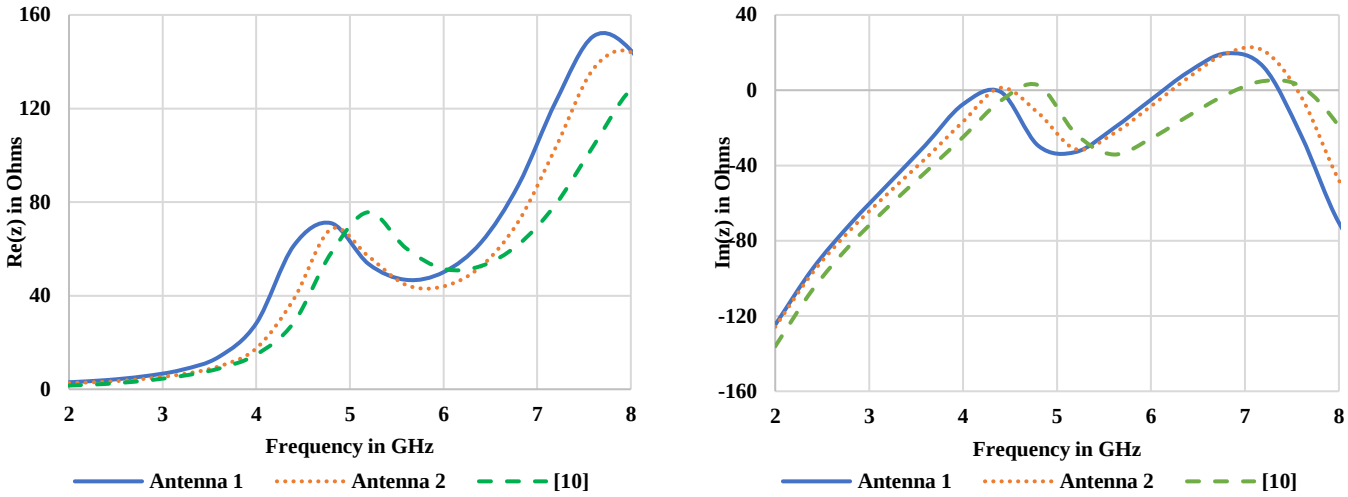

a) Re(Z) vs frequency plot for optimum geometries **b) Im(Z) vs frequency plot for optimum geometries**

Fig. 10 Impedance vs frequency characteristics for optimum geometries

The current distributions at three different frequencies are plotted for proposed antenna 1 and antenna 2 and are presented in Figure 11 (a, b, c) & (d, e, f), respectively. Further, these distributions are compared with the reference antenna shown in Figure 11 (g, h, i). From these diagrams, it may be noted that except at the starting frequency, the proposed antennas have better radiation characteristics than the reference antenna.

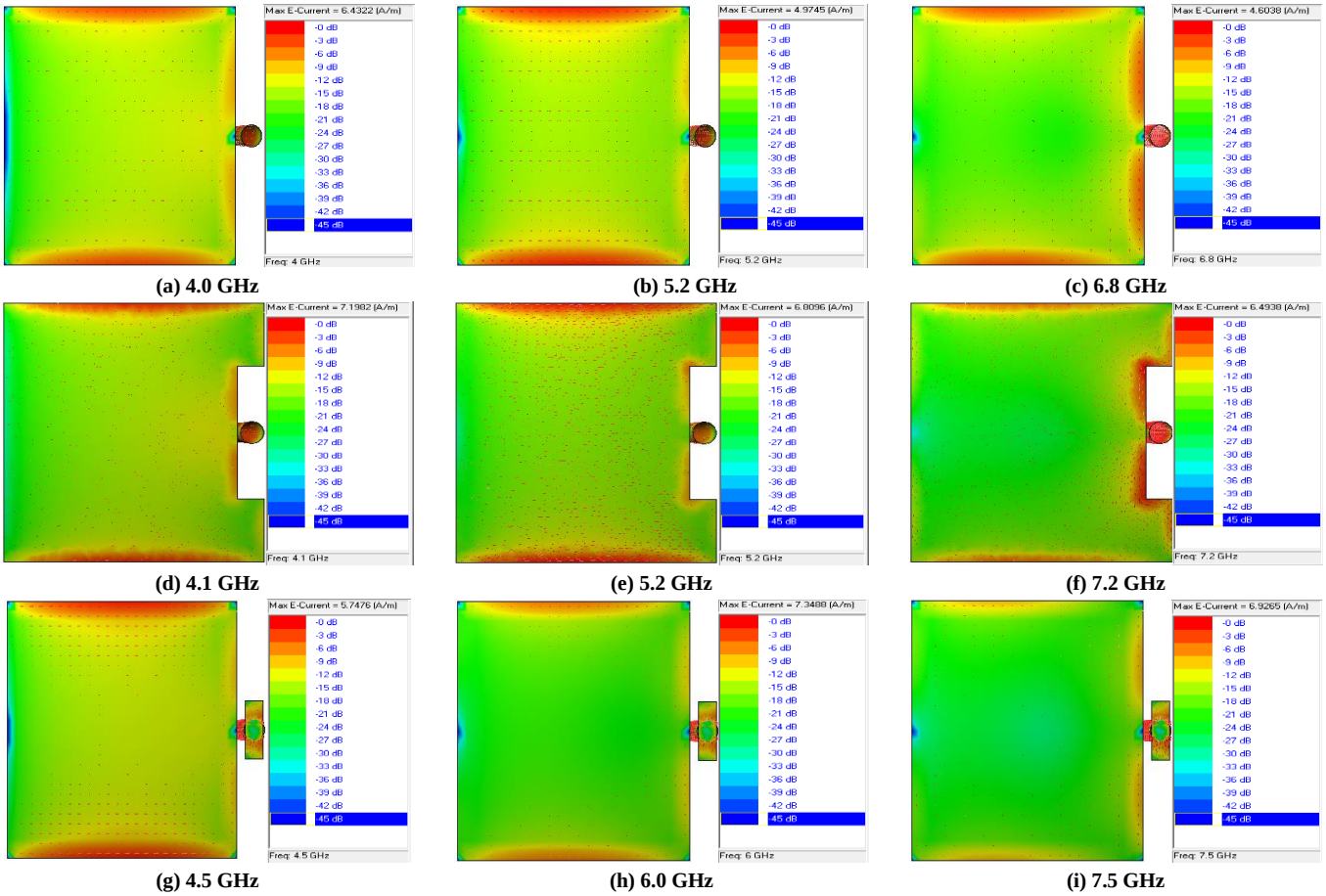

(a) 4.0 GHz **(b) 5.2 GHz** **(c) 6.8 GHz**

(d) 4.1 GHz **(e) 5.2 GHz** **(f) 7.2 GHz**

(g) 4.5 GHz **(h) 6.0 GHz** **(i) 7.5 GHz**

Fig. 11 Current distribution comparisons of proposed antennas with the reference antenna

4. Measured Results and Analysis

The antenna designs presented in Figure 2 & Figure 3 are fabricated, and a PNA network analyser (Agilent's PNA N5230A) was used to measure input characteristics. The dielectric material used for the design and development of the prototype is an FR4 with a permittivity of 4.4 and thickness of 1.6mm. The test antennas and their measurement setup are depicted in Figure 12. Simulated results are compared with the measured S_{11} characteristics (Figure 13). From these assessments, it must be noted that simulated data agree with the experimental values. The measured operational frequency band is from 4.08 GHz to 6.97 GHz for Antenna 1 and 3.82 GHz - 6.8 GHz for Antenna 2, equal to 52.30% and 56.12% return bandwidth values, respectively. Radiation characteristics were measured and plotted for both the proposed antennas at various frequencies across the band of operation (Figure 14 and Figure 15). The radiation plots depicted here exhibit that H-plane co-polarization radiation patterns are uniform at all frequencies. However, radiation plots are symmetrical at low-end frequencies for the E plane and become slightly asymmetrical at the high-frequency end. In all cases, the cross-polarization level at the bore-sight (0^0) angles was found to be better than -20 dB. The results of the proposed work are compared with similar works [10, 11, 31-37] available in the literature (pl. ref. Table 5). From Table 5, it may be noted that the present work is not only simple to optimize (due to the elimination of the feed strip) but also offers more bandwidth (above 50% in both cases) and good radiation patterns compared to the works existing in the literature.

(a) Antenna 1

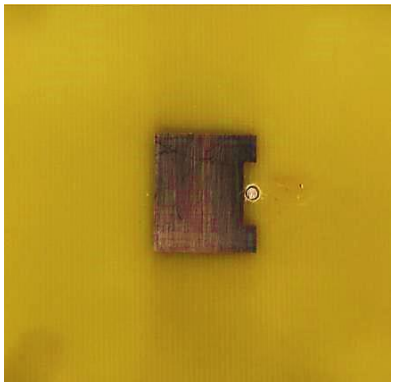

(b) Antenna 2

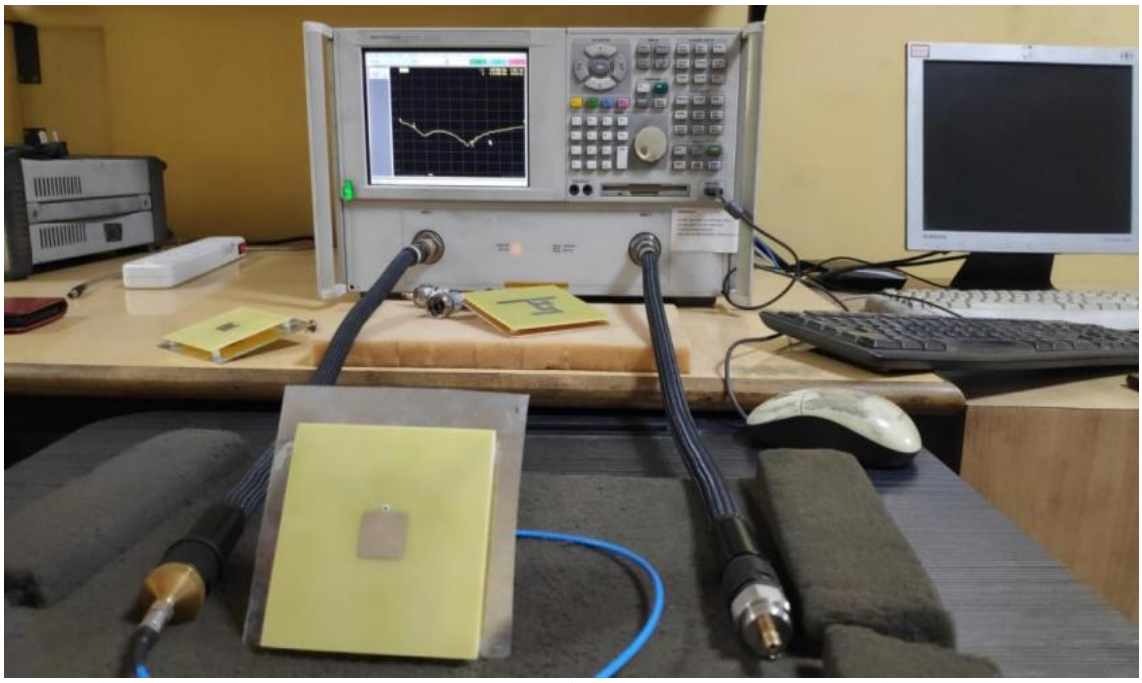

(c) Experimental setup for S_{11} characteristics

Fig. 12 Prototype antennas and their measurement setup

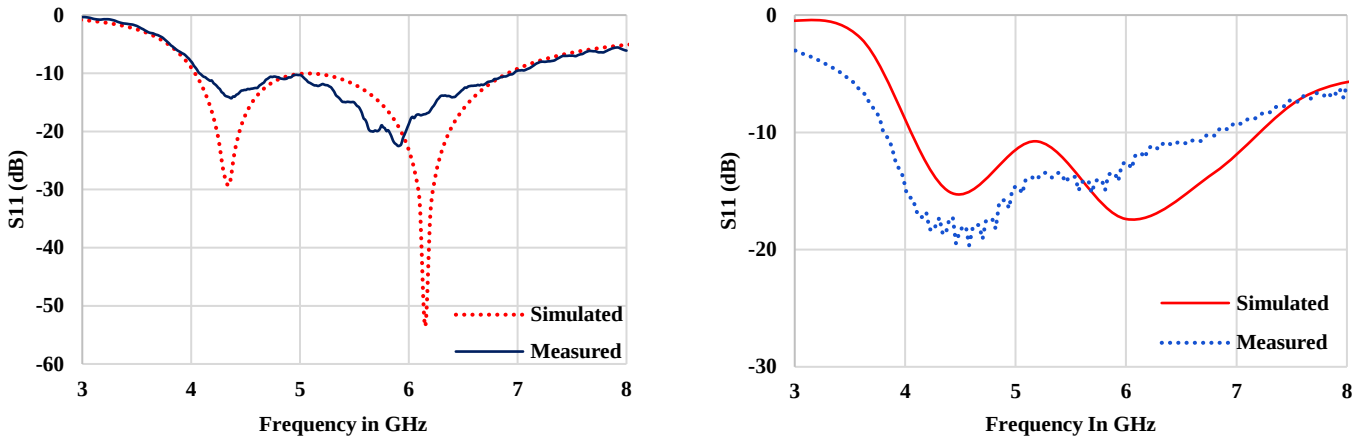

(a) S_{11} characteristics of antenna 1 (b) S_{11} characteristics of antenna 2

Fig. 13 Input impedance characteristics comparison of antennas 1 and 2

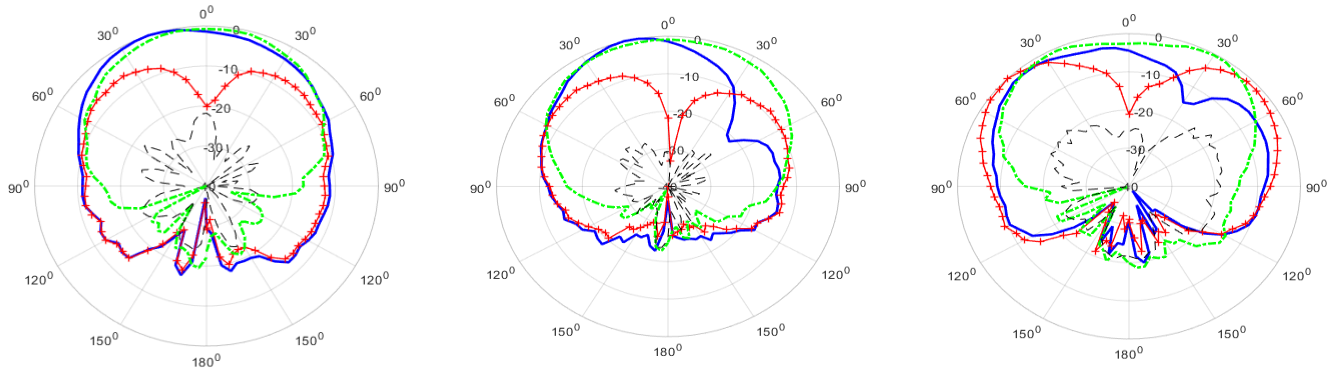

(a) 4.0 GHz (b) 5.2 GHz (c) 6.8 GHz

Fig. 14 Experimental radiation characteristics of the proposed antenna 1 at different frequencies. (Blue line (continuous): E-Co Polarization. (X-O-Z plane); Green curve (dash-dot): H-Co Polarization. (Y-O-Z plane); Red line with plus (+) curve: E-Cross Polarization.; Gray line (dashed): H-Cross Polarization.).
Note: Axes are as shown in Figures 2 and 3

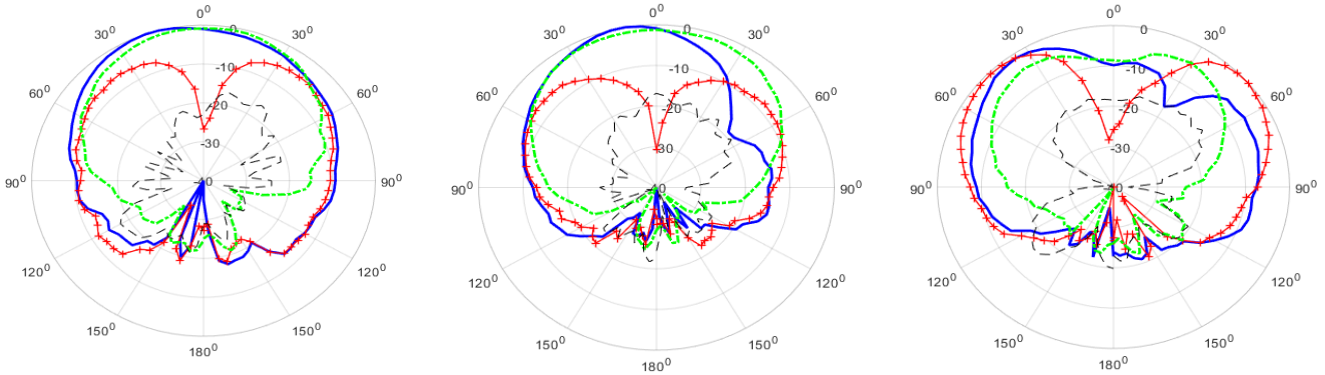

(a) 4.1 GHz (b) 5.2 GHz (c) 7.2 GHz

Fig. 15 Experimental radiation characteristics of the proposed antenna 2 at different frequencies. (Blue line (continuous): E-Co Polarization. (X-O-Z plane); Green curve (dash-dot): H-Co Polarization. (Y-O-Z plane); Red line with plus (+) curve: E-Cross Polarization.; Gray line (dashed): H-Cross Polarization.).
Note: Axes are as shown in Figures 2 and 3.

Table 5. Comparisons of proposed work with related work available in the literature

Ref. No.	Geometry shape	Type of feed strip	Operating frequency (f_c) or freq. range	Impedance Bandwidth (%)	Peak gain (%)
[10]	Rectangular	Rectangular	5.9GHz	50.7	7.15
[11]	Triangular (without truncation)	Rectangular (Vertex Feed)	3.57 GHz- 5.65 GHz	40.47	7.5
	Triangular (with truncation)	Rectangular (Vertex Feed)	3.57 GHz- 5.65 GHz	39.52	7.5
[16]	Hexagon with a rectangular slot	Rectangular	3.74 GHz-6.22GHz	49.79	--
[17]	Hexagon	Rectangular	4.42 GHz- 8.8 GHz	66.61 (Switch off)	6.5
	Hexagon	Rectangular	4.12 GHz- 8.91 GHz	68.42 (Switch on)	6.9
[33]	Square Ring	Circular	6.4 GHz	31.30	--
	Square Ring	Circular	6.23 GHz	23.60	--
[34]	Rectangular	Rectangular	1.8 GHz	26.40	8.2
	Circular	Rectangular	1.8 GHz	27.90	8.6
	Annular ring	Rectangular	1.8 GHz	26.10	8.5
[35]	H-shaped microstrip with U slot	Rectangular	5.1 GHz	46.00	5.4
[This work]	Rectangular (Antenna 1)	**- - (Eliminated)**	4.08 GHz-6.97 GHz	**52.3**	**6.92**
	Rectangular (Antenna 2)	**- - (Eliminated)**	3.82 GHz-6.8 GHz	**56.12**	**6.91**

5. Conclusion

Gap-coupled microstrip antennas with suspended configurations required for 5G & UWB communication systems were analyzed, fabricated, and measured. A new feed technique proposed here does not require any physical connection to the antenna element. Of the two antenna geometries proposed here offer a return loss bandwidth value of 52.3% and 56.12%, respectively. In both cases presented here, a proper match between the measured & simulated data was obtained. From the results presented here, it may be noted that the present work is not only simple to optimize (due to the elimination of the feed strip) but also offers more bandwidth (above 50% in both cases) and a good gain of 6.9dBi. The feed presented here is simple and needs only two parameters to be varied, i.e., d (separation parameter) and g (airgap), for the best possible bandwidth. Radiation parameters with stable characteristics across the band of operation have been obtained. With the results obtained here, the presented antenna geometries with novel feed are useful for 5G (lower band), long-term evolution (LTE), and other state-of-the-art ultrawideband systems.

Acknowledgement

The authors thank Prof. Vinoy K. J. (Chairman), Electrical Communication Engineering, IISc, Bengaluru and his research students, Mr. Aritra Roy & Mr. Anu Augustine, for their help during the antenna parameters measurements. The authors would also like to thank the Dept. of Sci. & Tech. (DST), GoK (KSTePS) for assisting grant/fellowship and carrying out this research work. The authors also would like to thank Dr. Rajeev Joshi, Physics Dept. CUK for providing Network Analyzer for cross-verification of results.

References

[1] Hao Zhang, and Ying-Zeng Yin, "Single-layer Single-feed Wideband Omnidirectional Microstrip Antenna with Rotating Square Patches," *Progress in Electromagnetics Research Letters*, vol. 93, pp. 27-34, 2020. *Crossref*, http://dx.doi.org/10.2528/PIERL20030301

[2] Wan-Jun Yang, Yong-Mei Pan, and Xiu-Yin Zhang, "A Single-layer Low-profile Circularly Polarized Filtering Patch Antenna," *IEEEAntennas and Wireless Propagation Letters*, vol. 20, no. 4, pp. 602-606, 2021. *Crossref*, https://doi.org/10.1109/LAWP.2021.3058790

[3] Syed S. Jehangir, and Mohammad S. Sharawi, "A Compact Single-layer Four-port Orthogonally Polarized Yagi-like MIMO Antenna System," *IEEE Transactions on Antennas and Propagation*, vol. 68, no. 8, pp. 6372-6377, 2020. *Crossref*, https://doi.org/10.1109/TAP.2020.2969810

[4] Ketavath Kumar Naik et al., "Design of Flexible Parasitic Element Patch Antenna for Biomedical Application," *Progress in Electromagnetic Research M*, vol. 94, pp. 143-153, 2020. *Crossref*, http://dx.doi.org/10.2528/PIERM20030406

[5] Haq Nawaz, and Muhammad Abdul Basit, "Single Layer, Dual Polarized, 2.4GHz Patch Antenna with Very High RF Isolation between DC Isolated Tx-Rx Ports for Full Duplex Radio," *Progress in Electromagnetic Research Letters*, vol. 85, pp. 65-72, 2019. *Crossref*, http://dx.doi.org/10.2528/PIERL19032806

[6] Zabed Iqbal, Tanzeela Mitha, and Maria Pour, "A Self-nulling Single-layer Dual-mode Microstrip Patch Antenna for Grating LobeReduction," *IEEE Antennas and Wireless Propagation Letters*, vol. 19, no. 9, pp. 1506-1510, 2020. *Crossref*, https://doi.org/10.1109/LAWP.2020.3007903

[7] Veeresh G. Kasabegoudar, and Pradeep Reddy, "A Review of Low-profile Single Layer Microstrip Antennas," *International Journal of Electrical and Electronic Engineering & Telecommunications*, vol. 11, no. 2, pp. 122-131, 2022. *Crossref*, http://dx.doi.org/10.18178/ijeetc.11.2.122-131

[8] Wangyu Sun et al., "Dual-Band Dual-Polarized Microstrip Antenna Array Using Double-Layer Gridded Patches for 5G Millimeter-Wave Applications," *IEEE Transactions on Antennas and Propagation*, vol. 69, no. 10, pp. 6489-6499, 2021. *Crossref*, https://doi.org/10.1109/TAP.2021.3070185

[9] Divya Soundharya et al., "Design of Ultra Wide Band Antenna," *SSRG International Journal of Electronics and Communication Engineering*, vol. 5, no. 6, pp. 7-10, 2018. *Crossref*, https://doi.org/10.14445/23488549/IJECE-V5I6P102

[10] Veeresh G. Kasabegoudar, and K. J. Vinoy, "Coplanar Capacitively Coupled Probe Fed Microstrip Antennas for Wideband Applications," *IEEE Transactions Antennas Propagation*, vol. 58, no.10, pp.3131-3138, 2010. *Crossref*, https://doi.org/10.1109/TAP.2010.2055781

[11] Veeresh G. Kasabegoudar, Dibyant S. Upadhyay, and K. J. Vinoy, "Design Studies of Ultra-wideband Microstrip Antennas with a Small Capacitive Feed," *International Journal of Antennas Propagation*, 2007. *Crossref*, https://doi.org/10.1155/2007/67503

[12] M. R. Solanki, K. Usha Kiran, and K. J. Vinoy, "Broadband Designs of Triangular Microstrip Antenna with a Capacitive Feed," *Journalof Microwaves, Optoelectronics, and Electromagnetic Applications*, vol. 7, no. 1, pp. 44-53, 2008.

[13] Veeresh G. Kasabegoudar, and K.J. Vinoy, "A Wideband Microstrip Antenna with Symmetric Radiation Patterns," *Microwave and Optical Technological Letter*, vol. 50, no.8, pp.1991-1995, 2008. *Crossref*, https://doi.org/10.1002/mop.23575

[14] Huaxiao Lu et al., "Capacitive Probe Compensation-fed Wideband Patch Antenna with U-shaped Parasitic Elements for 5G/WLAN/Wi-Max Applications," *IEICE Electronics Express*, vol. 16, no. 16, pp. 1-6, 2019. *Crossref*, https://doi.org/10.1587/elex.16.20190362

[15] Pradeep Reddy, and Veeresh G. Kasabegoudar, "A Novel Feeding Technique for Gap Coupled Suspended Ultra-wideband MicrostripAntennas," *IEEE Global Conference on Computing, Power and Communication Technologies (GLOBCONPT-2022)*, pp. 1-3, 2022. *Crossref*, https://doi.org/10.1109/GlobConPT57482.2022.9938152

[16] Tanaji D. Biradar, K. T. V. Reddy, and Kishor B. Biradar, "Circular Polarized MSA with Capacitive Fed and Shorting Pin," *Conference Emerging Devices and Smart Devices (ICEDSS 2017)*, pp. 142-145, 2017. *Crossref*, https://doi.org/10.1109/ICEDSS.2017.8073697

[17] Dinesh Kumar Singh et al., "Reconfigurable Circularly Polarized Capacitive Coupled Microstrip Antenna," *International Journal of Microwave and Technologies*, vol. 9, no. 4, pp. 843-850, 2016. *Crossref*, https://doi.org/10.1017/S1759078716000611

[18] Dinesh Kumar Singh et al., "Modeling of a Dual Circularly Polarized Capacitive-coupled Slit Loaded Truncated Microstrip Antenna," *Journal of Computational Electronics*, vol. 19, pp. 1564-1572, 2020. *Crossref*, https://doi.org/10.1007/s10825-020-01527-0

[19] Jiexi Yin et al., "Broadband Symmetrical E-Shaped Patch Antenna with Multimode Resonance for 5G Millimeter-Wave Applications,"*IEEE Transactions on Antennas and Propagation*, vol. 67, no. 7, pp. 4474-4483, 2019. *Crossref*, https://doi.org/10.1109/TAP.2019.2911266

[20] Amit A. Deshmukh, Divya Singh, and K.P. Ray, "Modified Designs of Broadband E-shape Microstrip Antennas," *Sādhanā*, vol. 44, 2019. *Crossref*, https://doi.org/10.1007/s12046-018-1030-8

[21] Ramesh Kumar Verma, and D.K. Srivastava, "Bandwidth Enhancement of a Slot Loaded T-shape Patch Antenna," *Journal of Computational Electronics*, vol. 18, pp. 205–210, 2019. *Crossref*, https://doi.org/10.1007/s10825-018-1277-7

[22] Abir Zaidi et al., "Compact Size T-Shaped Patch Antenna for E-Band Applications," *2019 International Conference on Wireless Networks and Mobile Communications (WINCOM-2019)*, pp. 1-3, 2019. *Crossref*, https://doi.org/10.1109/WINCOM47513.2019.8942527

[23] Sudhanshu Belwal, Ahmad Rafiquee, and Vibhor Bangwal, "Modified UWB Antenna for Cognitive Radio Applications," *SSRG International Journal of Industrial Engineering*, vol. 5, no. 3, pp. 15-18, 2018. *Crossref*, https://doi.org/10.14445/23499362/IJIE-V5I3P103

[24] C. L. Mak et al., "Experimental Study of a Microstrip Patch Antenna with an L-shaped Probe," *IEEE Transactions on Antennas and Propagation*, vol. 48, no. 5, pp. 777-783, 2000. *Crossref*, https://doi.org/10.1109/8.855497

[25] Shuo Yang et al., "A Dual-frequency Broadband Patch Antenna with L-shaped Probe Feed for 5G Communication," *2019 International Symposium on Antennas and Propagation (ISAP-2019)*, pp. 1-3, 2019.

[26] Pratigya Mathur, and Mahima Arrawatia, "Linear Microstrip Antenna Array with Reduced Patch Size Using L-shaped Probe for Electrically Thick Substrates," *2019 IEEE Indian Conference on Antennas and Propagation (InCAP-2019)*, pp. 1-4, 2019. *Crossref*, https://doi.org/10.1109/InCAP47789.2019.9134664

[27] Khanet Pookkapund et al., "Broadband Circularly Polarized Microstrip Patch Antenna using Circular Artificial Ground Structure and Meandering Probe," *IEEE Access*, vol. 8, pp. 173854-173864, 2020. *Crossref*, https://doi.org/10.1109/ACCESS.2020.3026166

[28] Wei-Jun Wu et al., "A Higher-order Mode Air-patch Antenna with a T-shape Feed," *2021 International Applied Computational Electromagnetics Society (ACES-China) Symposium*, pp. 1-2, 2021. *Crossref*, https://doi.org/10.23919/ACES-China52398.2021.9581960

[29] Veeresh G. Kasabegoudar, "Analysis of Coplanar Capacitive Coupled Wideband Microstrip Antenna," *International Journal of Engineering Trends and Technology*, vol 69, no. 9, pp. 45-50, 2021. *Crossref*, https://doi.org/10.14445/22315381/IJETT-V69I9P206

[30] Veeresh Gangappa Kasabegoudar, and Sarala Shirabadagi, "Quasi Yagi Antennas for State-of-the-Art Applications," *International Journal of Engineering Trends and Technology*, vol 70, no. 4, pp. 1-14, 2022. *Crossref*, https://doi.org/10.14445/22315381/IJETT-V70I4P201

[31] Pravin Dalvadi, and Amrut Patel, "Investigation and Analysis of High Gain Printed Curved Shape Director-Driven Bowtie Quasi-Yagi Antenna," *International Journal of Engineering Trends and Technology*, vol. 70, no. 7, pp. 301-309, 2022. *Crossref*, http://dx.doi.org/10.14445/22315381/IJETT-V70I7P231

[32] Pranav Bhatt et al., "Microstrip-Fed 3.04 -10.77 GHz UWB Patch Antenna Design Using CMA and Parametric Study," *InternationalJournal of Engineering Trends and Technology*, vol. 70, no. 7, pp. 250-259, 2022. *Crossref*, https://doi.org/10.14445/22315381/IJETT-V70I7P225

[33] Saidu Adamu Abubakar et al., "Characterization of Modified Electromagnetic Band Gap Structures for Notch Band Applications,"*SSRG International Journal of Electrical and Electronics Engineering*, vol. 7, no. 7, pp. 16-19, 2020. *Crossref*, https://doi.org/10.14445/23488379/IJEEE-V7I7P104

[34] M. A. Gonzalez de Aza, J. Zapata, and J. A. Encinar, "Broad-band Cavity-backed and Capacitively Probe-fed Microstrip Patch Arrays," *IEEE Transactions on Antennas Propagation*, vol. 48, no. 5, pp. 784-789, 2000. *Crossref*, https://doi.org/10.1109/8.855498

[35] G. Mayhew-Ridgers, J.W. Odondaal, and J. Joubert, "Single-layer Capacitive Feed for Wideband Probe-fed Microstrip Antenna Elements," *IEEE Transactions on Antennas Propagation*, vol. 51, pp. 1405-1407, 2003. *Crossref*, https://doi.org/10.1109/TAP.2003.812186

[36] Vaibhav Tarange et al., "A U Slotted H-shaped Microstrip Antenna with Capacitive Feed for Broadband Application," *2011 International Conference on Emerging Trends in Networks and Computer Communications (ETNCC)*, pp. 182-184, 2011. *Crossref*, https://doi.org/10.1109/ETNCC.2011.5958511

[37] S. A. Arunmozhi, and V. Benita Esther Jemmima, "A High Gain Ultra Wideband Array Antenna for Wireless Communication," *International Journal of Recent Engineering Science*, vol. 7, no. 6, pp. 31-34, 2020. *Crossref*, http://ijresonline.com/archives/IJRES-V7I6P105